

Supporting Information

Content

S1. Raman Date

S2. The surface elemental composition

S3. A comparison of ORR performance of PFCMs–1000
with other catalysts

S4. The morphology of PDCFs

S5. The hollow distribution of dopamine pyrolysis

S6. The elemental composition of PFCMs–1000

S7. Differ concentration of ORR performance
in alkaline medium

S8. The specific surface area and pore size distribution

S9. The morphology of PFCMs–1000 after stability test

References

S1. Raman Date

Table S1. Peak positions and integrated intensity (I_D/I_G) of NCS.

Samples	G band(cm^{-1})	D band(cm^{-1})	I_D/I_G
NCS-700	1593.49	1325.73	2.30
NCS-800	1592.70	1328.84	2.33
NCS-900	1591.49	1336.49	2.60
NCS-1000	1590.49	1346.73	2.77

S2. The surface elemental composition

Table S2. Summary of the surface elemental composition as determined by XPS

Sample	XPS (%)			
	Fe	C	N	O
PFCMs-1000	2.87	80.94	5.26	12.18
CPDCFs	1.6	49.90	2.15	45.07

S3. A comparison of ORR performance of PFCMs-1000 with other catalysts

Table S3. Summary of reported ORR performance for nonprecious-metal-doped carbon catalysts in alkaline media (0.1 M KOH)

Sample	Mass loading (mg cm ⁻²)	Onset Potential (V vs. RHE)	Kinetic current Density (mA cm ⁻²)	Ref.
PFCMs-1000	0.24	0.949	-6.21 (@ 0.6 V)	This work
Fe-N-CNFs	0.60	0.93	-4.85 (@ 0.5V)	1
N-Fe-C@CNTs	0.09	0.88	-	2
Fe-N/C	0.10	0.92	-7.4 (@ 0.82 V)	3
NHPCM-1000	0.32	0.88	-6.19 (@ 0.6 V)	4
N-OMCS-1.5-900	1.00	0.77	-	5
PANiD_O ₂ _800	0.48	0.75	-4.36 (@ 0.4V)	6
NMCS-3	0.66	0.86	-	7
Fe _{0.33} -CoP	1.65	0.90	-4.20 (@ 0.5V)	8
B ₁₂ C ₇₇ N ₁₁	0.2	0.96	-4.29 (@ 0.4 V)	9
Meso/micro-PoPD	0.50	0.90	-	10
TTF-F	0.3	0.86	-4.9 (@ 0.6 V)	11
NiCoP/CNF900	0.4	0.82	-7.19 (@ 0.4V)	12
BP-NFe	0.40	1.06	-	13
DG	0.08	0.91	-5.2 (@ 0.4 V)	14
NCFs	0.16	0.736	-3.3 (@ 0.23V)	15
N-doped graphene	0.05	0.95	-6.7 (@ 0.58 V)	16
NHPCM-1000	0.32	0.88	-6.19 (@ 0.6 V)	17
Pt/MPCNFs	0.30	0.99	-4.75 (@ 0.4V)	18
PANI-4.5Fe-T2(SBA-15)	-	0.95	-7.4 (@ 0.82 V)	19

S4. The morphology of PDCFs

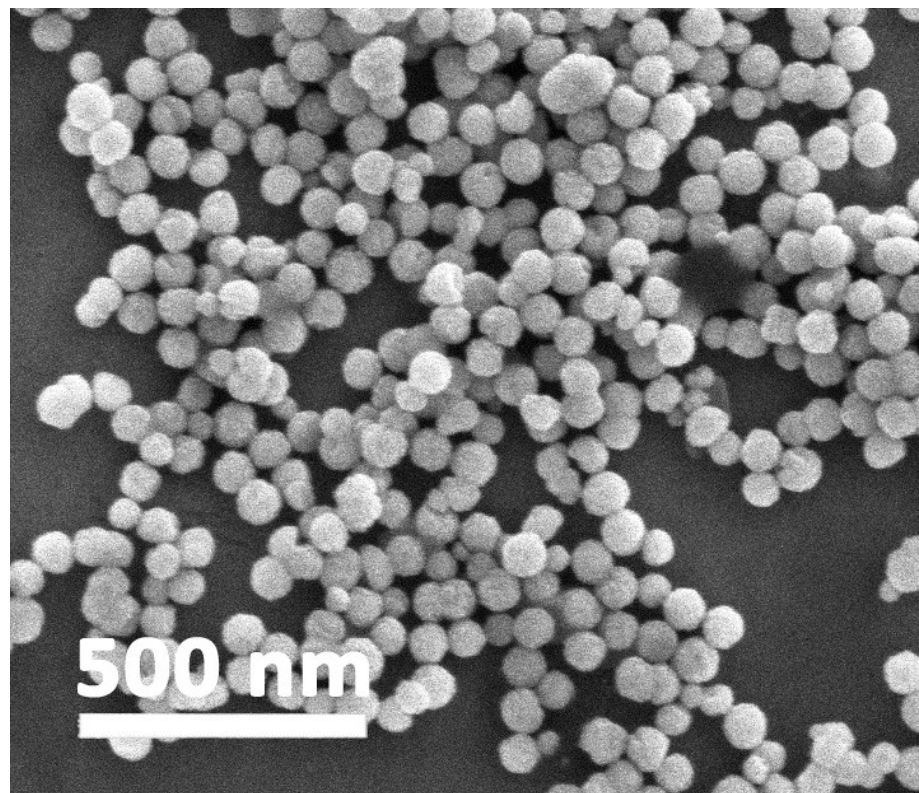


Fig. S1 SEM image of PDCFs.

S5. The surface hollow distribution of dopamine pyrolysis

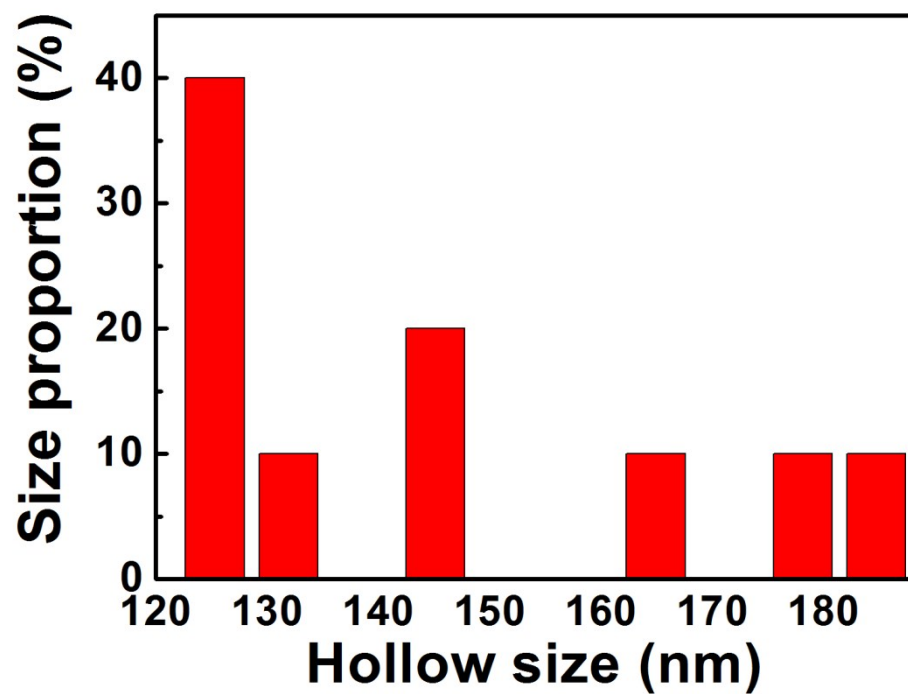


Fig. S2 The surface hollow size distribution histogram of PFCMs -1000.

S6. The elemental composition of PFCMs–1000

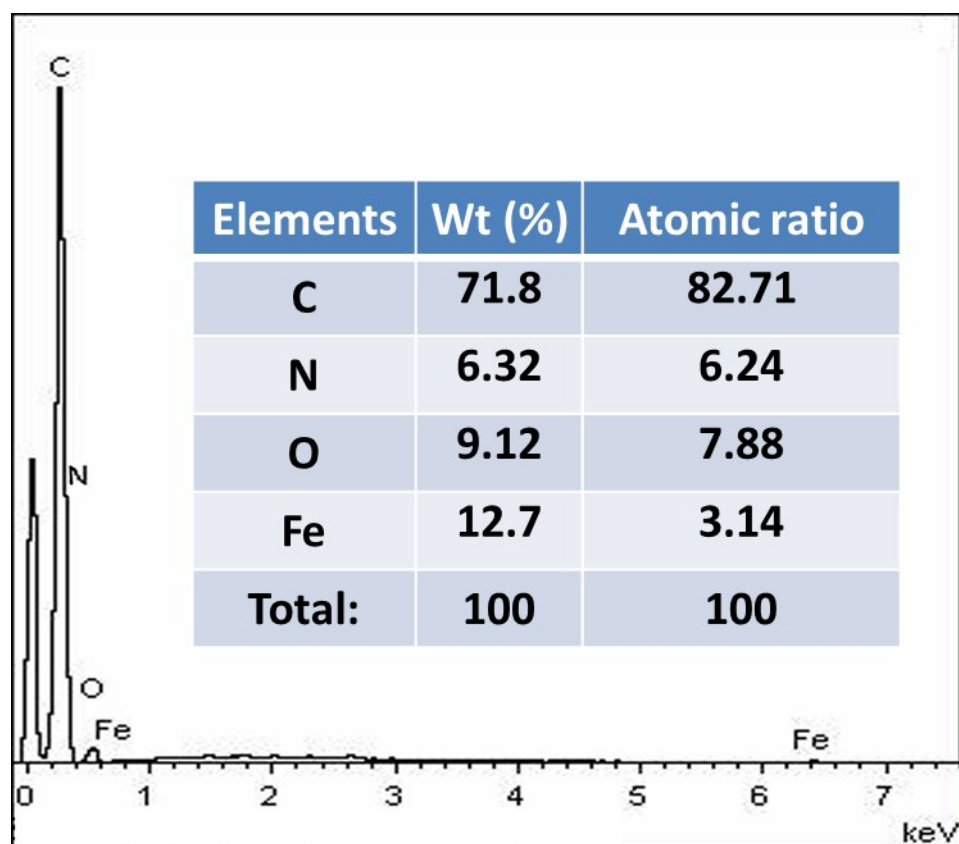


Fig. S3. EDX spectrum of PFCMs-1000.

S7. The specific surface area and pore size distribution

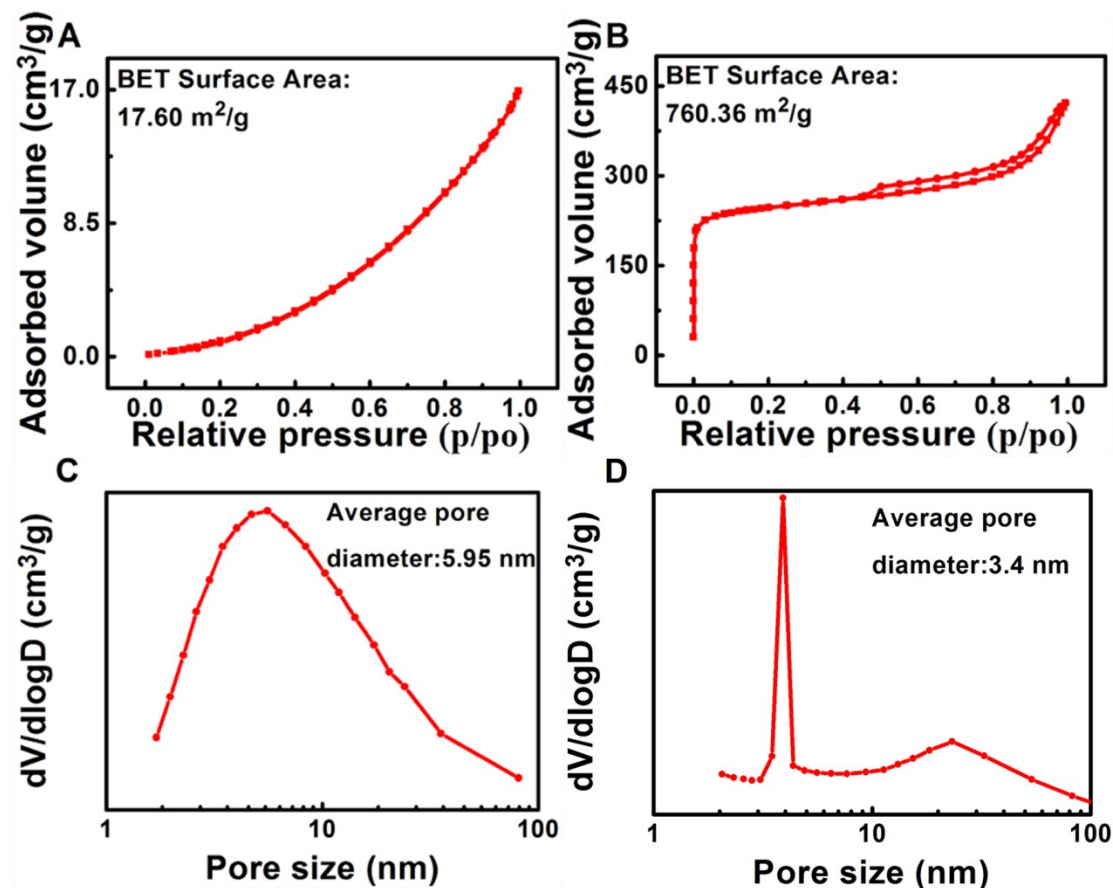


Fig. S4 The N₂ adsorption curve of (a) CPDCFs and (b) PFCMs-1000. The KJS pores size distribution of (c) CPDCFs and (d) PFCMs-1000.

S8. Differ concentration of ORR performance in alkaline medium

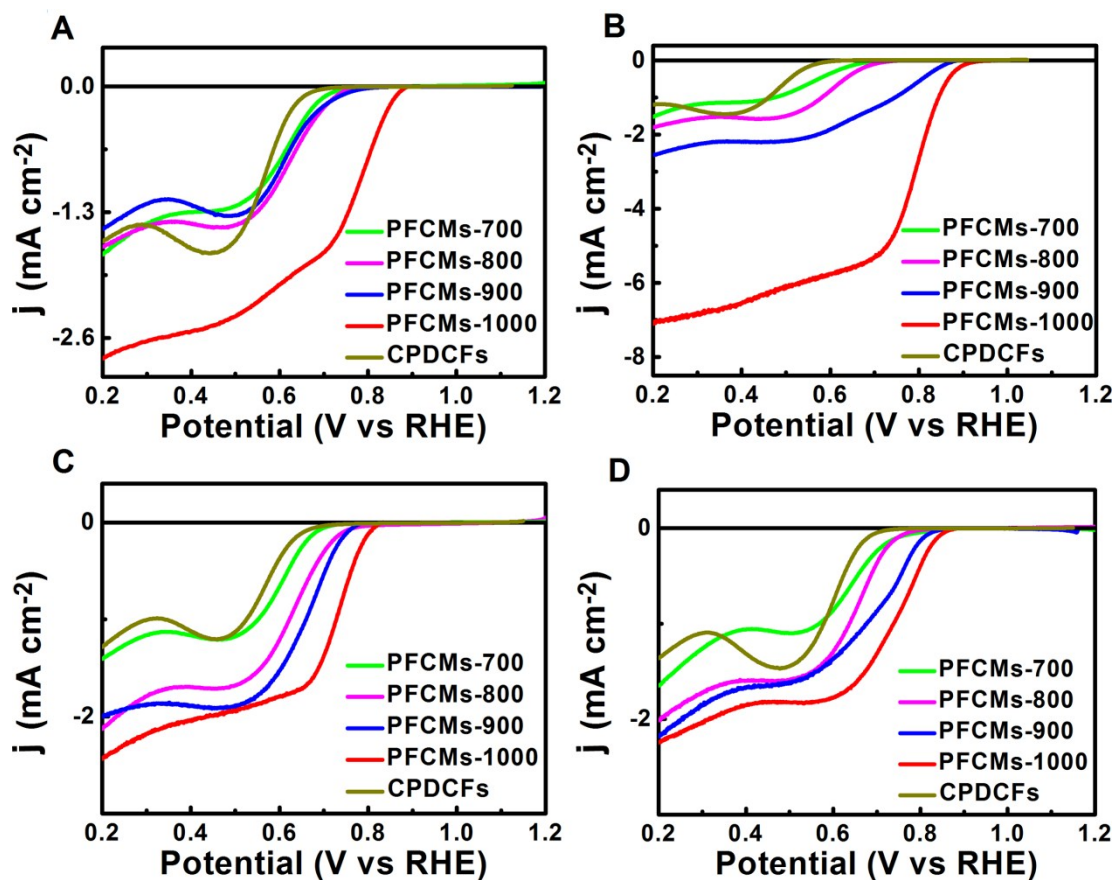


Fig. S5 The RDE polarization curves with synthesis concentration at (A) 0.2M (B) 0.3M (C) 0.4M and (D) 0.5M in changed temperature with a scan rate of 10 mV s^{-1} .

S9. The morphology of PFCMs–1000 after stability test

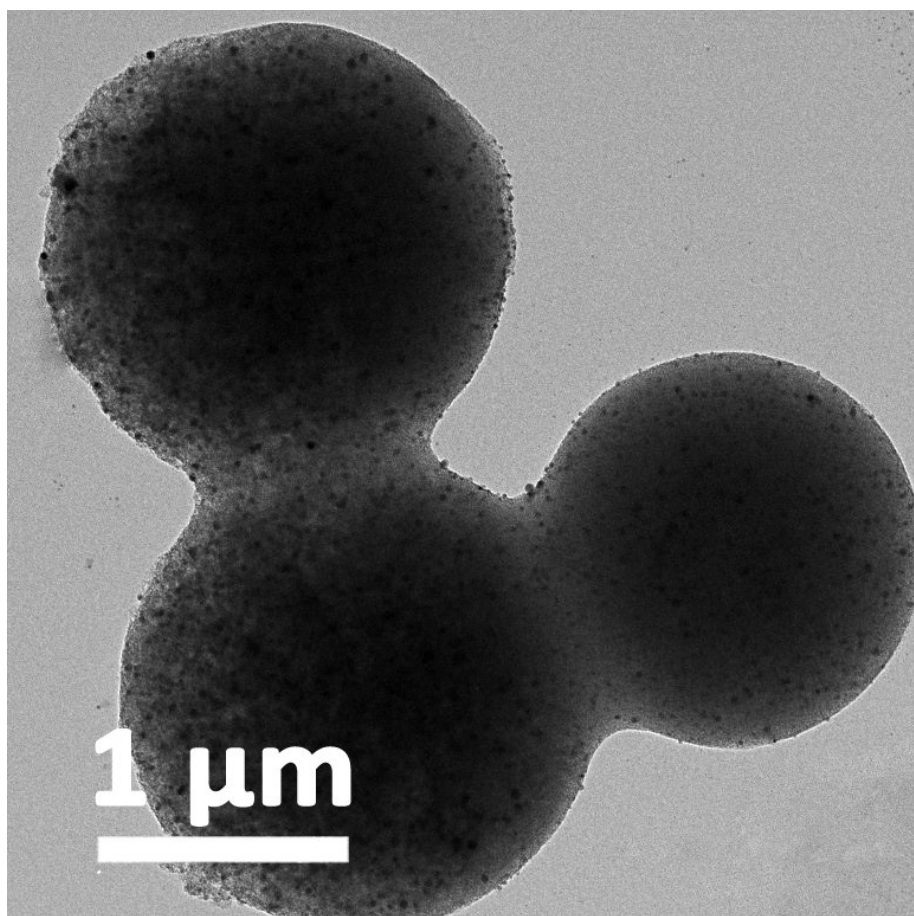


Fig. S6 TEM images of PFCMs–1000 after stability test.

References

- 1 Z. Y. Wu, X. X. Xu, B. C. Hu, H. W. Liang, Y. Lin, L. F. Chen, and S. H. Yu, *Angew. Chem., Int. Ed.*, 2015, **54**, 8179–8183.
- 2 C. Hu, L. Wang, Y. Zhao, M. Ye, Q. Chen, Z. Feng, and L. Qu, *Nanoscale*, 2014, **6**, 8002–8009.
- 3 L. Lin, Q. Zhu, and A.-W. Xu, *J. Am. Chem. Soc.*, 2014, **136**, 11027–11033.
- 4 Y. Chen, R. Ma, Z. Zhou, G. Liu, Y. Zhou, Q. Liu, S. Kaskel, and J. Wang, *Adv. Mater., Interfaces* 2015, **2**, 1500199.
- 5 J. Li, Z. Li, J. Tong, C. Xia, and F. Li, *RSC Adv.*, 2015, **5**, 70010–70016.
- 6 J. Quílez-Bermejo, C. González-Gaitán, E. Morallón, and D. Cazorla-Amorós, *Carbon*, 2017, **119**, 62–71.
- 7 J. Tang, J. Liu, C. Li, Y. Li, M. O. Tade, S. Dai, and Y. Yamauchi, *Angew. Chem. Int. Ed.*, 2015, **54**, 588–593.
- 8 X. Qin, Z. Wang, J. Han, Y. Luo, F. Xie, G. Cui, X. Guo and X. Sun, *Chem. Commun.*, 2018, **54**, 7693–7696.
- 9 S. Wang, L. Zhang, Z. Xia, A. Roy, D. W. Chang, J. B. Baek, and L. Dai, *Angew. Chem., Int. Ed.*, 2012, **51**, 4209–4212.
- 10 H.-W. Liang, X. Zhuang, S. Brüller, X. Feng, and K. Müllen, *Nat. commun.*, 2014, **5**, 4973.
- 11 L. Hao, S. Zhang, R. Liu, J. Ning, G. Zhang, and L. Zhi, *Adv. Mater.*, 2015, **27**, 3190–3195.
- 12 S. Surendran, S. Shanmugapriya, A. Sivanantham, S. Shanmugam, and R. K. Selvan, *Adv. Energy Mater.*, 2018, **20**, 1800555.
- 13 J. Liu, X. Sun, P. Song, Y. Zhang, W. Xing, and W. Xu, *Adv. Mater.*, 2013, **25**, 6879–6883.
- 14 Y. Jia, L. Zhang, A. Du, G. Gao, J. Chen, X. Yan, C. L. Brown, and X. Yao, *Adv. Mater.*, 2016, **28**, 9532–9538.
- 15 C. Xu, S. Chen, L. Du, C. Li, X. Gao, J. Liu, L. Qu, and P. Chen, *ACS Sustainable Chem. Eng.*, 2018, **6**, 3358–3366.
- 16 K. Parvez, S. B. Yang, Y. Hernandez, A. Winter, A. Turchanin, X. Feng, and K. Müllen, *ACS nano*, 2012, **6**, 9541–9550.
- 17 Y. Chen, R. Ma, Z. Zhou, G. Liu, Y. Zhou, Q. Liu, S. Kaskel, and J. Wang, *Adv. Mater. Interfaces*, 2015, **2**, 1500199.
- 18 K. K. Karuppanan, A. V. Raghu, M. K. Panthalingal, S. Ramanathan, T. Kumaresan and B. Pullithadathil, *J. Mater. Chem. A*, 2018, **6**, 12768–12781.
- 19 X.-H. Yan and B.-Q. Xu, *J. Mater. Chem. A*, 2014, **2**, 8617–8622.